Nanoscale Self-Organization Using Standing Surface Acoustic Waves

Christophe Taillan, Nicolas Combe, and Joseph Morillo

Centre d'Elaboration de Matériaux et d'Etudes Structurales, CNRS UPR 8011, 29 rue J. Marvig, BP 94347, 31055 Toulouse cedex 4, France and Université de Toulouse; UPS; F-31055 Toulouse, France

(Received 25 June 2010; published 18 February 2011)

The diffusion of an adatom on a substrate submitted to a standing surface acoustic wave is theoretically studied. By performing large scale molecular dynamic simulations, we show that the wave dynamically structures the substrate by encouraging the presence of the adatom in the vicinity of the maximum displacements of the substrate. Using an analytical model, we explain this feature introducing an effective potential induced by the wave. Applied in an atomic deposition experiment, this dynamic structuring process should govern the nucleation sites distribution opening the route to accurately control the self-organization process at the nanoscale.

DOI: 10.1103/PhysRevLett.106.076102 PACS numbers: 68.35.Fx, 05.65.+b, 68.35.Iv

Besides industries that resort to many stages in the fabrication of microelectronic devices [1], many laboratories try to benefit from the self-organizing properties of materials at the nanoscale. Atomic self-organization approaches, especially during molecular beam epitaxy of semiconductors, are usually based on the elastic and/or structural properties of deposited and substrate materials: (i) the Stranski-Krastanov growth mode approach relies on the competition between surface and elastic energy to induce a 3D growth but provides a limited control of the self-organization [2]; (ii) in the technically delicate buried dislocation network approach, the self-organization is driven by the induced strain field at the free surface substrate [3]; (iii) the growth on prepatterned substrate surfaces has also been investigated but requires an expensive substrate preparation [4].

We propose here an alternative approach: the dynamic substrate structuring effect. At the macroscopic scale, a sand bunch can be organized on a drum by exciting one of its membrane modes of vibration. The vibrating drumhead is structured by the nodes and antinodes of vibration, which yield the self-organized behavior of the sand grains [5]. The efficiency of such an approach, though experimentally performed at the mesoscale [6,7] has never been evidenced nor investigated at the nanoscale.

We propose to use a standing surface acoustic wave (SSAW) at the surface of a substrate to control the adatoms diffusion in any atomic deposition process. The SSAW wavelengths of interest will be typically of the order of few to hundred nanometers (nm). Using atomic scale molecular dynamic simulations, we demonstrate the existence of this dynamic structuring effect induced by the SSAW on the atomic diffusion at the nanoscale and then give a theoretical description of this phenomenon.

Large scale molecular dynamics (MD) simulations of an adatom on a crystalline substrate submitted to a SSAW are performed with the LAMMPS code [8]. Figure 1 shows a sketch of the system under study. The SSAW propagates in the x direction, with wavelength λ, wave number k, and angular frequency Ω. The simulation cell is periodic in the x and y directions and made of 31 atomic planes in the z direction, with the diffusing adatom on the upper z atomic plane representing the surface of the substrate. Its size in the x direction varies from 2λ to 4λ, while in the y direction the size is fixed from the cutoff distance of the semiempirical potential. The 12 topmost atomic layers and the diffusing adatom evolve in the microcanonical ensemble. A Nose-Hover thermostat is applied to the 15 next atomic layers in order to simulate the thermostating effect of the underlying substrate and the last four layers are kept fixed to simulate its semi-infinite character. The SSAW is created by imposing a z-sinusoidal displacement to few substrate atoms localized around the $x = 4$ plane in the vicinity of the surface at a frequency close to a resonant excitation of a surface vibration mode: the SSAW results then from the periodic boundary conditions in the x direction. The energy injected in the system by this generation process is efficiently dissipated by the thermostat and the elastic energy induced by the SSAW does not alter the substrate crystallinity. The atoms interactions are of the Lennard-Jones (LJ)

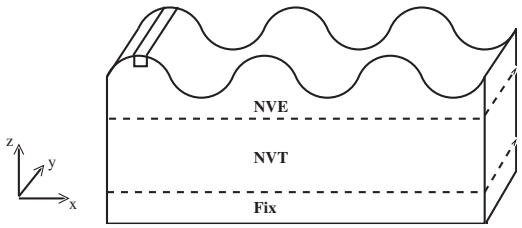

FIG. 1. Sketch of the simulation model used in the study. Atoms in the dashed region have an imposed vertical sinusoidal displacement (frequency Ω) and produce a SSAW along the x direction. Atoms in the vicinity of the surface are in the microcanonical ensemble, the atoms in the large intermediate region are coupled to a thermostat (canonical ensemble) and the four bottom layers of the substrate are kept fixed.

type [9]. The interaction parameters are $\epsilon = 1$ and $\sigma = 1$ for the substrate atoms (mass $m = 1$) where we have chosen the following units: times, distances, masses, energies, and temperatures are expressed in units of $\sqrt{\frac{\epsilon}{m\sigma^2}}$, σ, m, ϵ and ϵ/k (k, the Boltzmann constant). The structure is fcc with a $a = 1.587$ lattice parameter. The thermostat temperature is $T = 0.24$. The simulation cell orientation is that of the fcc lattice. The adatom (mass $m_a = m$)—substrate interaction is also LJ ($\epsilon_a = 0.82$ and $\sigma_a = 1$). These parameters discourage the adatom evaporation or exchange with substrate atoms on the simulation time scale, while insuring a significant diffusion on the (001) surface. The cell contains from 11 904 to 23 808 atoms and the simulations are typically performed on 4×10^6 steps of 2×10^{-3} time units. Such simulations would roughly correspond to a few nanoseconds at about 1000 K using typical energies, masses, and lattice spacings of noble metals [10]. Under these conditions, the SSAW characteristics are $\lambda = 38.1$ and $\Omega = 0.785$. We investigate the diffusion of a single adatom on a crystalline substrate submitted to a SSAW. The $z(x)$ displacement of the top substrate atomic layer induced by the SSAW is plotted in Fig. 2(d) at 2 times corresponding to antinodes maximum displacements. Figure 2(a) reports the x position (abscissa) of the diffusing adatom versus time (ordinate) with and without the SSAW. Without the SSAW, the adatom experiences a Brownian-like motion, while in its presence, it spends more time in the vicinity of the SSAW antinodes.

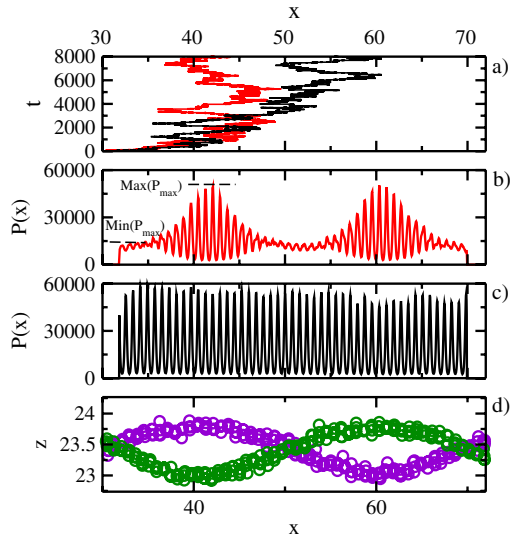

FIG. 2 (color online). LJ simulations at $T = 0.24$. (a) x position of the diffusing adatom (abscissa) as a function of time (ordinate) on a substrate submitted (red or gray) or not (black) to a SSAW. (b) and (c) $P(x)$ distribution of the x adatom coordinate over about a period λ of the SSAW: (b) with and (c) without the SSAW. (d) $z(x)$ displacement of the top of the substrate atomic layer at 2 times corresponding to antinode maximum displacements. The cell x size for these simulations is 2λ.

To evidence this potentially structuring effect, we perform a statistical study: we calculate $P(x)$, the distribution of the adatom x coordinate from 300 trajectories of about 8000 time units each, whose starting points were uniformly distributed along x.

Figure 2 reports $P(x)$ with (b) and without (c) the SSAW. The $P(x)$ distribution, in both cases, presents a short wavelength oscillation ($a/2$). This oscillatory behavior results from the periodic crystalline potential induced by the substrate. More importantly, the amplitude of the oscillations are almost constant in the absence of the SSAW, whereas in its presence their envelop is periodic at half the wavelength λ of the SSAW [Figs. 2(b) and 2(d)]: a clear evidence of the structuring effect of the SSAW. The amplitudes of the oscillations are maximum at the antinodes and about 4 times larger than around the nodes of the SSAW; the SSAW, thus, significantly increases the probability to find the adatom in the vicinity of its antinodes.

This structuration can be interpreted in terms of an effective energy difference at the mesoscopic λ scale between the node and antinodes which can be deduced from these $P(x)$ curves: $\Delta E^{\text{eff}}_{\text{SSAW}} = k_b T \ln[\max(P_{\max})/\min(P_{\max})]$, with $P_{\max}$ the ensemble of local maxima of $P(x)$ and max (min) the ensemble maximum (minimum). From Fig. 2, $\Delta E^{\text{eff}}_{\text{SSAW}} = 1.44kT$, i.e., ≈ 120 meV for a LJ noble metal at 1000 K.

Since true interatomic potentials in crystalline materials are much more complex than a simple LJ potential, we have simulated a more realistic adatom diffusion, namely, the diffusion, at $T = 600$ K, of a silver adatom on a (001) silver surface with the embedded atom method (EAM) potential [11]. Because of the heavy computational cost of these simulations (26 785 atoms in the cell), we only

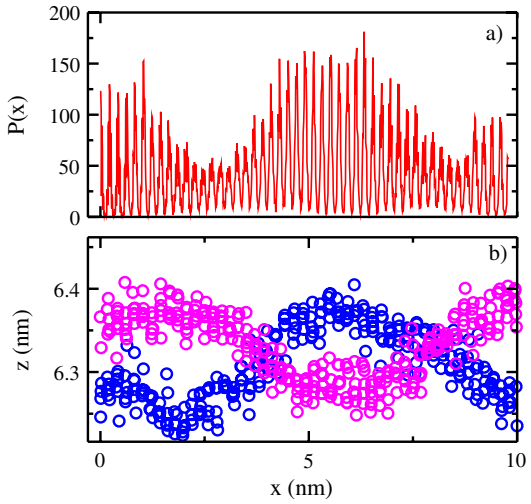

FIG. 3 (color online). Silver EAM-potential simulations at $T = 600$ K. (a) $P(x)$ distribution of the x adatom coordinate over about a period λ of the SSAW in the presence of the SSAW. (b) Same as Fig. 2(d). $T = 600$ K. The cell x size for these simulations is 3λ.

report in Fig. 3, the $P(x)$ distribution in the presence of the SSAW, calculated from 48 trajectories of 90 ns. Figure 3 confirms the conclusions established with the simple LJ potential: the $P(x)$ distribution is enhanced in the vicinity of the SSAW antinodes. The less pronounced structuring effect of the SSAW with the EAM potential than with the LJ potential, results from the poorer statistics and the difference between bonding energies and induced SSAW forces. From Fig. 3, we measure $\Delta E_{\mathrm{SSAW}}^{\mathrm{eff}} = 1.14kT = 59$ meV.

In order to understand the structuring effect, we perform a spectral analysis of the force acting on the adatom. Figure 4(a) reports $\tilde{F}(x, \omega)$, the time Fourier transform of $F(x, t)$, the x component of the force acting on the adatom at position x. The $F(x, t)$ values were collected as the $P(x)$ values, but along low temperature ($T = 0.05$) LJ trajectories [12]. This low temperature was imposed in order to reduce the adatom diffusion and the thermal noise [13]. Pronounced peaks in the spectrum clearly appear at $\Omega = 0.82$, the SSAW angular frequency [14]. Smaller peaks also show up at multiples of the SSAW frequency. The comparison between the x dependence of the Fourier coefficients of the force at the SSAW frequency [Fig. 4(b)], and the z displacement of the top substrate atomic layer [Fig. 4(c)] reveals that this force is periodic in space at the wavelength of the SSAW and in a quadrature relationship with it. The effect of the SSAW on the adatom appears therefore essentially as a force field periodic in time and space at the frequency and wavelength of the SSAW and in quadrature with it. The intensity of this force field depends on the precise substrate-adatom interaction, and on the SSAW amplitude.

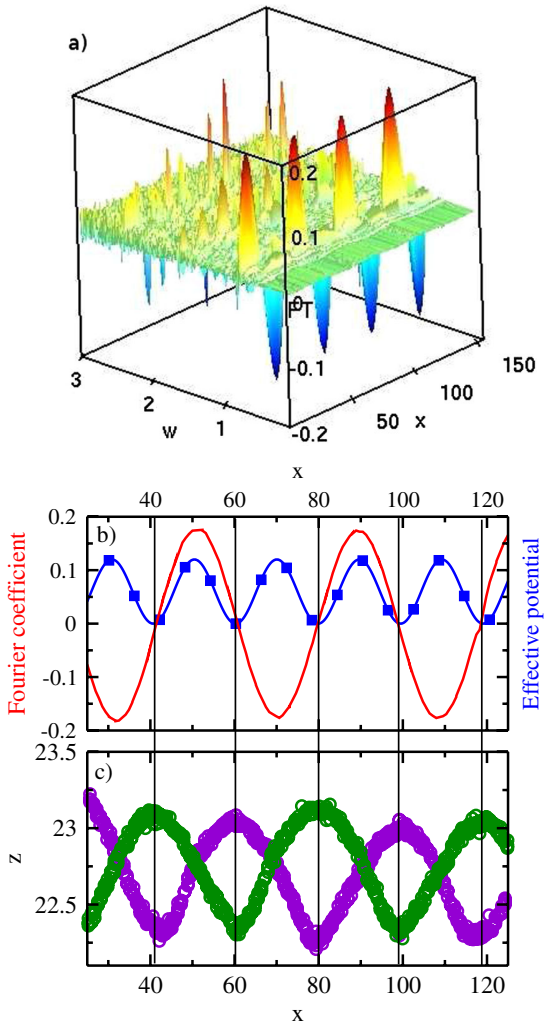

FIG. 4 (color online). LJ simulations at $T = 0.05$. (a) $\tilde{F}(x, \omega)$, time Fourier transform of $F(x, t)$ as a function of the angular frequency and adatom position. (b) (red curve) $\tilde{F}(x, \Omega = 0.82)$ as a function of the adatom position. (blue square curve) Effective potential (arbitrary unit) calculated from Eq. (4). (c) Same as Fig. 2(d). Vertical black lines are guides to the eyes.

Indeed it is related to the curvature of the surface induced by the SSAW (a Rayleigh wave [15]) which gives rise to a local time dependent strain field. The longitudinal component of this strain field $\epsilon_{xx}(x, t)$ induces a stretching (shortening) of the substrate bond distances at maxima (minima) of the SSAW displacements, leading to a lower (higher) adatom adsorption energy, but also to a modulation of the static activation barrier for diffusion [16,17]. Both effects contribute to the observed modulations of the $P(x)$ curves (Figs. 2 and 3). These modulations of the potential experienced by the adatom give then rise to a SSAW force in quadrature with the displacement of the surface [Fig. 4(b)].

A model description of the x-coordinate adatom movement, under the influence of the SSAW, can be given through a Langevin type equation. A theoretical derivation of such an equation and its detailed study, will be given in a forthcoming publication. We here concentrate on the most relevant terms: the SSAW force and the friction force. The adatom motion equation writes

$$m_a\ddot{x} + \gamma\dot{x} = F\cos(\Omega t)\sin(kx), \tag{1}$$

where the SSAW force is modeled by its fundamental Fourier component $F\cos(\Omega t)\sin(kx)$, and the thermal damping force by a viscous force with γ an effective friction coefficient. Following Landau and Lifshift [15], solutions of Eq. (1) can be decomposed into the sum of a slowly varying function of time $X(t)$ and a fast oscillating term $\zeta(t)$ (at frequency Ω): $x(t) = X(t) + \zeta(t)$. Inserting this decomposition in Eq. (1) and developing to the first order in ζ, we established the two following equations by separating the fast oscillating and the slow varying terms.

$$m_a\ddot{\zeta} + \gamma\dot{\zeta} = F\cos(\Omega t)\sin(kX(t)), \tag{2a}$$

$$m_a\ddot{X} + \gamma\dot{X} = \overline{\zeta(t)Fk\cos(\Omega t)\cos(kX(t))}. \tag{2b}$$

In Eq. (2b), the overline corresponds to an average time value over one period of the fast oscillation. Injecting solutions of Eq. (2a) at constant $X(t)$, in Eq. (2b), yields

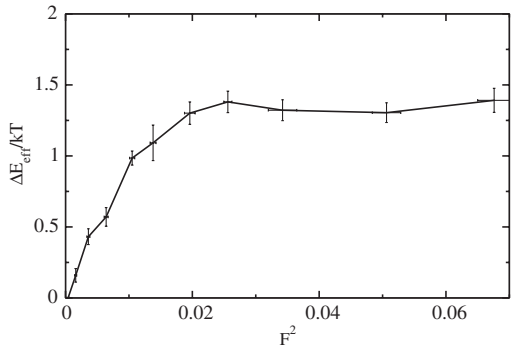

FIG. 5. LJ simulations at $T = 0.24$. $\Delta E^{\text{eff}}_{\text{SSAW}}$ as function of the squared SSAW induced force. Values of $\Delta E^{\text{eff}}_{\text{SSAW}}$ and F are, respectively, deduced from $P(x)$ diagrams analogous to Fig. 2(b) and analogous data to the ones of Fig. 4.

$$m_a\ddot{X} + \gamma\dot{X} = -\frac{F^2 k m_a}{2(m_a^2\Omega^2 + \gamma^2)}\cos(kX)\sin(kX). \quad (3)$$

The second member of Eq. (3) is a time independent effective force at the mesoscopic time scale ($t \gg 2\pi/\Omega$) that derives from an effective potential $U_{\text{eff}}(X)$:

$$U_{\text{eff}}(X) = \frac{F^2 m_a}{4(m_a^2\Omega^2 + \gamma^2)}\sin^2(kX). \quad (4)$$

Variations of $U_{\text{eff}}(X)$ (in arbitrary units) are reported on Fig. 4(b), showing the good agreement between our model and the atomic scale simulations. The minima of the effective potential and the structuring effect of the SSAW occur at half the wavelength of the SSAW and at its antinodes. $U_{\text{eff}}(X)$ appears as governing the long time evolution ($t \gg 2\pi/\Omega$) of the "mean" position of the adatom.

This effective potential and the structuring energy $\Delta E^{\text{eff}}_{\text{SSAW}}$ which both govern the structuration must be related and thus an F^2 dependence of $\Delta E^{\text{eff}}_{\text{SSAW}}$ is expected in the small forces region where the previous perturbative calculation sounds well. This is what we do observe as shown on Fig. 5.

Using MD simulations and analytical models, we have evidenced that a SSAW on a crystalline surface structures the diffusion of adatoms.

Going beyond this result, if several adatoms diffuse on the substrate, as during atomic deposition experiments, we expect the SSAW to organize the nucleation of solid germs. The key difficulty for a practical implementation of the proposed dynamic structuring process is the generation of SSAWs on a substrate. Wavelengths of SAW produced using an electromechanical system (typically interdigital transducers) are about hundreds of nm or more despite some developments in order to produce high SAW frequencies (and small wavelengths) [18]. Nanopatterned surfaces optically excited have succeeded in producing SAW with 125 nm wavelength [19]. Finally, let us mention the growing interest these last years in the production of Tera-hertz (bulk) phonons [20]. None of the above techniques can presently produce SSAWs with nm wavelengths to test our prediction. However, the dynamic structuring mechanism does not depend on the SSAW wavelength (though its strength may) and may thus be considered using tens or hundred nm wavelength SSAW.

The dynamic structuring process is a very versatile structuring technique. Using several SSAWs, square or triangular 2D networks could be obtained at the nanoscale: the number, wave vectors direction [6,21], and wavelengths of SSAW control the position and density of nanostructures.

We believe that the proposed dynamic structuring process will likely constitute a clever way to control the self-organization in atomic deposition processes to produce 2D periodic networks of 3D structures in a single stage.

This work was performed using HPC resources from CALMIP (Grant No. 2010-1022) and from CINES. We thank A. Ponchet for her critical reading of the manuscript.

[1] K. Galatsis *et al.*, Adv. Mater. **22**, 769 (2010).
[2] A. Zangwill, *Physics at Surfaces* (Cambridge University Press, Cambridge, 2009).
[3] H. Brune *et al.*, Nature (London) **394**, 451 (1998).
[4] A. Turala *et al.*, Appl. Phys. Lett. **94**, 051109 (2009).
[5] I. S. Aranson and L. S. Tsimring, Rev. Mod. Phys. **78**, 641 (2006).
[6] J. Shi *et al.*, Lab Chip **9**, 2890 (2009).
[7] M. Dorrestijn *et al.*, Phys. Rev. Lett. **98**, 026102 (2007).
[8] S. J. Plimpton, J. Comput. Phys. **117**, 1 (1995).
[9] The pair potential energy between two atoms separated by a distance r writes $U = 4\epsilon[(\sigma/r)^{12} - (\sigma/r)^6]$.
[10] P. Guan, D. R. Mckenzie, and B. A. Pailthorpe, J. Phys. Condens. Matter **8**, 8753 (1996).
[11] S. M. Foiles, M. I. Baskes, and M. S. Daw, Phys. Rev. B **33**, 7983 (1986).
[12] 192 independent trajectories of 650 time units each.
[13] x positions of the adatom in Fig. 4 have been discretized and correspond to minima of the crystalline potential.
[14] The angular frequency of SSAW slighlty depends on the temperature: 0.82 at $T = 0.05$ versus 0.785 at $T = 0.24$.
[15] L. D. Landau and E. M. Lifshitz, *Theory of Elasticity* (Pergamon Press, Oxford, 1986); *Mechanic* (Mir, Moscow, 1969), 3rd ed.
[16] C. Ratsch, A. P. Seitsonen, and M. Scheffler, Phys. Rev. B **55**, 6750 (1997).
[17] M. Schroeder and D. E. Wolf, Surf. Sci. **375**, 129 (1997).
[18] Y. Takagaki *et al.*, Semicond. Sci. Technol. **19**, 256 (2004).
[19] M. E. Siemens *et al.*, Appl. Phys. Lett. **94**, 093103 (2009).
[20] A. J. Kent *et al.*, Phys. Rev. Lett. **96**, 215504 (2006).
[21] T. Sogawa *et al.*, Appl. Phys. Lett. **91**, 141917 (2007).